

THE MARCI WATER ICE CLOUD OPTICAL DEPTH (PUBLIC) DATABASE

M. J. Wolff, *Space Science Institute, Boulder, CO, USA* (mjwolff@spacescience.org), **R. T. Clancy**, *Space Science Institute, Boulder, CO, USA*, **B. Cantor**, *Malin Space Science Systems*, **R. M. Haberle**, *NASA/Ames Research Center*.

Introduction: The presence of ice clouds in the Martian atmosphere was originally inferred from their color contrast with the “yellow hazes” observed in early telescopic photographs. The specific identification of water ice resulted from analysis of Mariner 9 IR spectra of clouds over the Tharsis ridge [1]. The image datasets compiled by the Mariner 9 and the Viking orbiters characterized the general morphology and large-scale (qualitative) behavior of Martian water ice clouds. While these analyses offered insight into the physical forms taken by clouds and their association with meteorological (and dynamical) phenomena, they were viewed primarily as passive tracers or probes of more fundamental atmospheric behavior. This picture has changed in part due to advances in photochemical and dynamical modeling of the Martian climate, as well as the influx of new data from the renaissance of Mars spacecraft observations that began with the arrival of Mars Global Surveyor (MGS) in 1997; and continued with the subsequent Mars Odyssey, Mars Express, and Mars Reconnaissance Orbiter (MRO) missions.

No past or currently-active spacecraft missions to Mars have flown without some type of imaging system. Nevertheless, the Mars Observer Camera (MOC, [2]) onboard MGS is the first example of an imager that routinely provided global-scale observations over a very short timescale (i.e., a day). The limited number of studies that have directly exploited the synoptic monitoring capabilities of MOC may be understood in terms of the difficulties associated with retrieving water ice properties (e.g., photometric calibration, spatially dependent surface properties, dust-ice discrimination). However, the arrival of the Mars Color Imager (MARCI, [3]) onboard MRO offers an alternative (though complementary in temporal coverage) source of data that overcomes the primary limitations of MOC. Specifically, MARCI possesses more precise a radiometric calibration and offers a UV channel that emphasizes the contributions of water ice clouds while minimizing those associated with dust and surface properties (and their uncertainties). As such, the MARCI data directly provide for the generation of “daily global maps” (DGMs) of water ice optical depth for use in dynamical modeling studies and atmospheric remote sensing (i.e., gas abundance) retrievals.

The goal of this presentation is to 1) provide an update of the algorithms involved that have occurred

since the previous description, e.g., [4]; 2) briefly describe the end-products of the DGM retrieval process, including several example applications; and 3) advertise the public repository of the water ice retrieval products currently available.

Relevant MARCI Dataset Details:

The MARCI instrument and its performance/calibration have been described elsewhere, including the the UV channels [3,4,5]. The specific details relevant to the water ice retrievals are involve “Band 7”, which has a centroid of 321 nm, a radiometric accuracy of ~6-8%, and a radiometric precision of 2-3%. The intrinsic spatial sampling of Band 7 provides near-global daily coverage at ~8 km/pixel (nadir). The “near” qualification for coverage stems from the fact MRO’s orbit is too low to spatially contiguous optical depth values (outside of the polar regions).

Algorithm Updates: The current version of processing algorithm is essentially that described by [6], with two exceptions: 1) the use of CRISM-based zonal dust climatology; and 2) the implementation of surface reflectance property map. Here, we briefly describe these two updates.

CRISM Dust Climatology. Dust is one of the quantities that must be prescribed as part of the cloud retrieval process. Analyzing the approximately 20,000 emission phase function (EPF) observations made by the Compact Reconnaissance Imaging SpectroMeter (CRISM, [7]) with the retrieval algorithm of [8], one can construct a database of “concurrent” dust optical depths. As can be seen in Figure 1, the coverage offered by this EPF dataset contains temporal and spatial gaps even within a zonal-bin representation. To provide geographical coverage (i.e., transform zonal value to a particular longitude), we scale the dust optical depths from the 0-elevation surface to that of a given MARCI pixel using a constant-mixing, exponential atmosphere approximation (10 km scale height). For MARCI data acquired after the end of EPF acquisitions (stopped due to a gimbal problem), an average dust value is derived from the database for a given latitude and L_S (but excluding those for the MY 28 global dust event). A text version of the complete EPF dataset is available upon request from the first author.

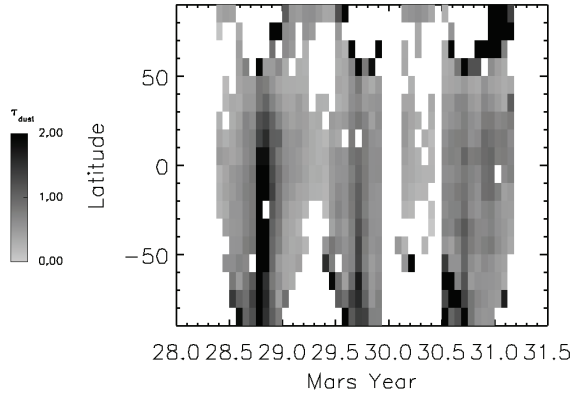


Figure 1. Zonal dust map derived from CRISM EPF measurements, scaled to the 0-elevation surface.

Fortunately, the errors associated with the dust column prescription are minimized by the weak dependence of the derived water ice column on this parameter for all but the lowest ice loading conditions. This can be seen in Figure 2, which shows the Band 7 (model) radiance (I/F) as a function of dust and ice optical depths. The “flatness” of the isophotes is an indication of this general insensitivity for $\tau_{\text{dust}} \geq \sim 0.05$ -0.1. As such, the use of CRISM (versus the Thermal Emission Spectrometer climatology [9]) represents an attempt to improve the MARCI retrieval precision for low ice conditions.

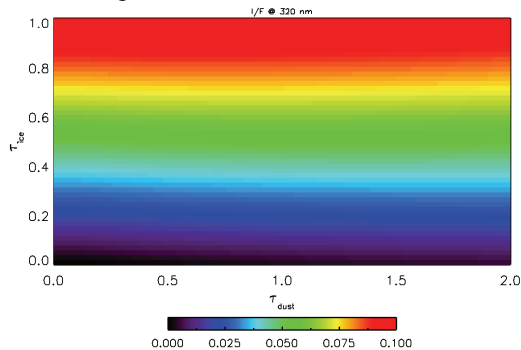


Figure 2. Model normalized radiance (I/F) levels for Band 7 as a function of dust and water ice optical depth. The flatter the isophote contour, the weaker the dependence of the ice optical depth on a particular dust optical depth.

Surface reflectance map. A primary advantage of the MARCI Band 7 (versus MOC-Blue) is the low absolute surface reflectance and the (expected) more muted nature of its spatial variations. Using the spatially uniform surface properties of [6], one can observe patterns of water ice cloud opacity that appear to correlate with visible surface albedo features. This occurs primarily for lower dust loading conditions, suggesting the general limitation of the uniform surface approximation. However, the associated water ice optical depths are quite small, typically less than 0.03. As a result, this “improvement” is targeted at the precision of the MARCI retrieval for low ice conditions.

Ignoring the potential for diminishing returns, we created a version of the MARCI mapping retrieval that returns the Hapke function “w” parameter. Employing 4 separate multi-week periods (and locations) where we expected/observed an absence of clouds, we combined the resulting “w” retrievals to produce a global map. Even with averaging, it was necessary to mask out regions around the volcanoes and to apply a smoothing filter. As can be seen in Figure 3, the results are quite striking, at least with respect to the *anti-correlation* with visible albedo features. There is nothing about the “w” retrieval input parameters (i.e., dust vertical profile, topography, etc.) that would produce this pattern if it was not present in the Band 7 images. In essence, Figure 3 appears to be a (noisy) map of the violet (or UV) contrast discussed by [10], though clearly it occurs at scales beyond those originally identified.

Ultimately, a small improvement is produced in the water ice optical depth values for low ice atmospheric conditions. However, a precise quantitative assessment of this improvement is still underway.

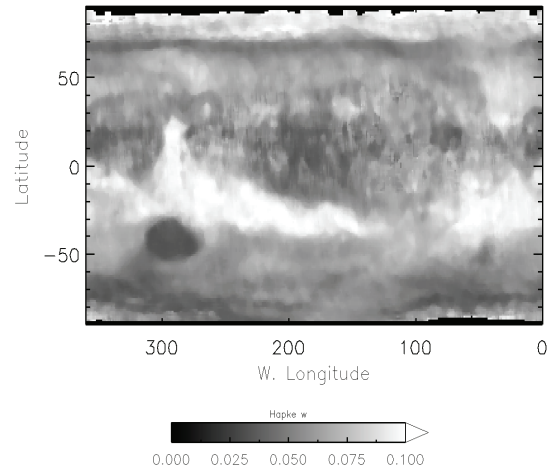


Figure 3. Map of the Band 7 surface reflectance through the use of the “w” parameter of the Hapke function. Notice the anti-correlation with visible albedo features, the so-called violet/UV contrast reversal, e.g., [10]. Western Longitude convention used.

Basic Retrieval Products: For every mapping day (for which observations are obtained), a water ice cloud optical depth image and associated metadata “backplanes” are produced, corresponding pixel-by-pixel to each MARCI image “strip.” (12-13 per day). An example of the coverage can be seen Figure 4, which is the map-projected “mosaic” all the “tau” strips from day 222 of 2010 ($L_S=131^\circ$, MY 30). This mosaic also highlights the weakness of the current retrieval in that surface ice is retrieved as cloud opacity. Such pixels are flagged (but not eliminated) in the polar region during a post-processing step (using a seasonally dependent cap-radius and the I/F values). This approach allows the tabulation of optical depth values without the need to depend on detailed validity of cap location algorithm. The

potential for confusion due to surface ice outside of the polar regions remains present (e.g., in craters or the floor of Hellas).

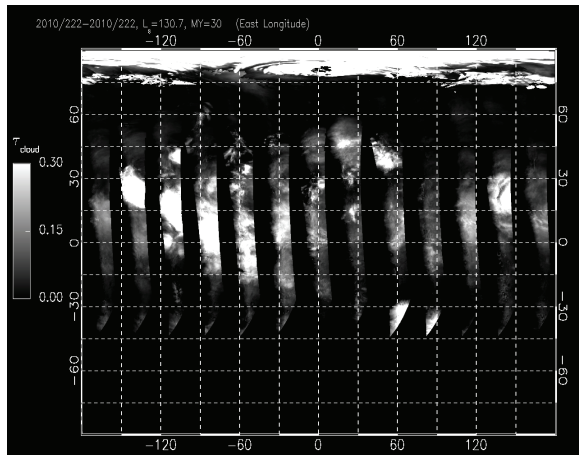


Figure 4. Daily Global Map (mosaic) of the water ice cloud optical depths for a representative aphelion season "day" ($L_s=131^\circ$, MY 30). Eastern Longitude convention used. The opacity associated with polar cap highlights the limitation of the current retrieval algorithm over icy surfaces. We attempt to flag such pixels in a post-processing step while leaving the retrieved values intact to avoid the need to reprocess for different polar cap "models."

A basic database of MARCI retrievals is constructed by including every valid retrieval pixel (including potential polar cap pixels) and the associated metadata for that pixel (e.g., ephemeris time, atmospheric state variables like surface pressure, dust column; photometric angles; local time). The database key is composite and involves (time, longitude, latitude). Each included "tau" pixel is a unique record. However, the resulting dataset (at the native resolution) is > 60 GB for all retrievals through the end of MY 31, even when stored as compressed (scaled) integers. To make a more tractable product, one can choose a lower resolution spatial mesh. Binning the retrievals for each mapping day on a $1^\circ \times 1^\circ$ spatial grid results in database size of ~ 1 GB (compressed). In addition, higher-level datasets/products can be constructed easily by searching the database and potentially "binning" the query results. In the next sections, we provide several examples of such higher-level products and briefly describe the public data products (including their location).

Example Applications/Products..

Annual/Interannual Variations. A zonally averaged quantity is often used to assess annual and interannual trends and variations. An example of this for the MARCI water ice retrieval is shown in Figure 5 (top). Starting with the $1^\circ \times 1^\circ$ database, the data are further down-sampled to 5° latitude and 5-

day temporal bins. The anticipated large-scale phenomena are clearly present, e.g., aphelion cloud belt, polar hoods. One's eye can pick up slight differences in the annual cycle from year-to-year. A more quantitative assessment of such variations can be obtained by removing a "mean" behavior from each year. The bottom panel of Figure 5 illustrates the results of such a subtraction, where the "mean" year is the average of MY 30 and 31. This simple exercise highlights potential differences in water ice cloud activity in the period leading up to and in the year after the MY 28 global dust event. Currently, we are investigating these variations in a more systematic (i.e., detailed) manner.

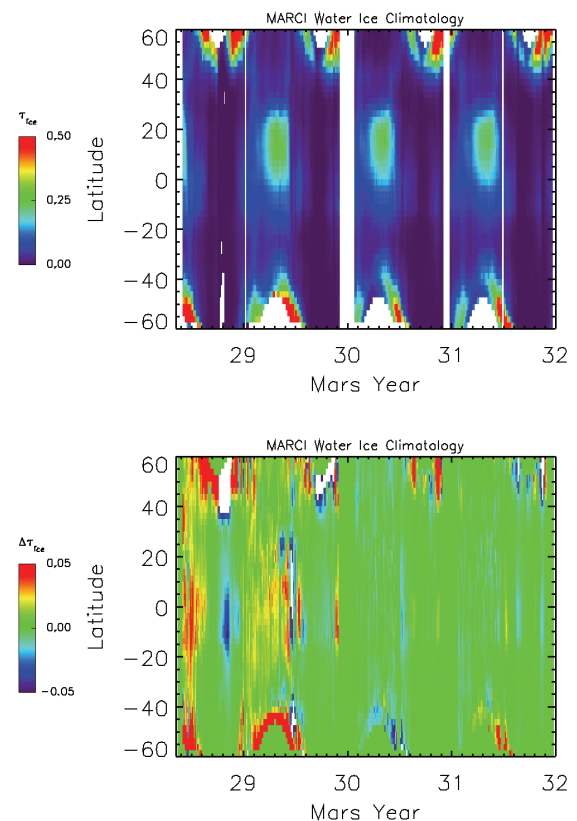


Figure 5. Top panel illustrated the zonally-averaged water ice optical history through the end of MY 31. The lower plot illustrates the difference in the optical depth history with respect to an average "year" (constructed from MY 30 and 31). Blue indicates less dust than the average year while red reveals the presence of more. In the top panel, white represents "missing data" (i.e., polar night); unfortunately, this is captured in the bottom panel as a "0" level or no difference.

Spatially resolved patterns. The zonally-average data naturally suppresses any longitudinal structure in the water ice cloud behavior. A simple data product that avoids this limitation is a "snapshot" or temporal average on a spatial grid, where the scale of each is determined by the particular application. For example, Figure 6 compares Ames Global Climate Model (GCM) water ice columns to those of MARCI

water ice retrievals, where the latter is binned spatially to match the model resolution; both datasets are averaged over the season $L_S=315^{\circ}$ - 330° . The correspondence of the Wave-3 pattern between the observations and model provides a nice model validation (Ames GCM run 11.41), but the mismatch of optical depths simultaneously indicates a “problem.” Comparison runs with a new version of the GCM (using an updated microphysics package) are currently underway.

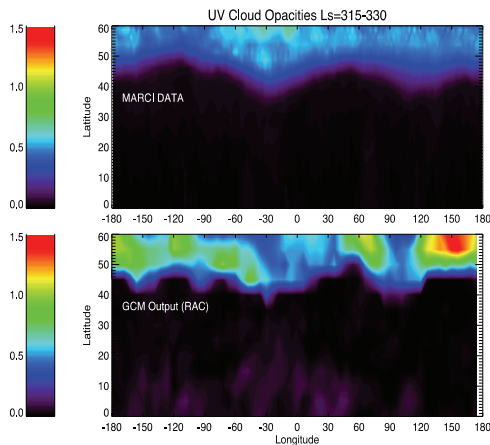


Figure 6. Comparison of water ice optical depths between MARCI and an Ames GCM simulation for the same season. The values for each dataset are plotted using an identical binning and dynamic range. The model calculations include radiative active clouds and are taken from Ames GCM run 11.41.

Point/Region Time-series. A final simple (but useful) product that we wish to highlight is that of a time-series for a (small) region of interest. Obvious applications of the ROI-level approach include the location of surface assets (e.g., coordinated observations) and of “interesting” dynamical activity (e.g., volcanoes). Figure 7 provides an example of each of these topics: the top panel for the Curiosity region and the bottom panel for the western flank of Arsia Mons. The error bars are meant to capture random (noise) errors and small-scale spatial variability. They were calculated during the generation of the $1^{\circ} \times 1^{\circ}$ database using simple sampling statistics for all MARCI “tau” pixels that fell with a given spatial bin for that mapping day. The scatter above this level represents actual day-to-day variability in the water ice cloud activity. The error associated with model input uncertainties is estimated to be below 0.03 for low-to-moderate ice optical depths. A more precise characterization of the error budget is ongoing.

Public Database: As of mid-December (2013), we are distributing water ice retrieval (and metadata) products through a Twiki portal hosted at the Space Science Institute:

<https://gemelli.space-science.org/twiki/bin/view/Mar>

[sObservations/MarciObservations/WaterIceClouds](https://gemelli.space-science.org/twiki/bin/view/MarciObservations/WaterIceClouds)).

This release includes data for MY 28-30 for the zonal and snapshot products. Current data formats are limited to NetCDF and text. In addition, basic documentation that describes the metadata fields is included, as will be a preprint of the retrieval algorithm publication (as soon as it is available).

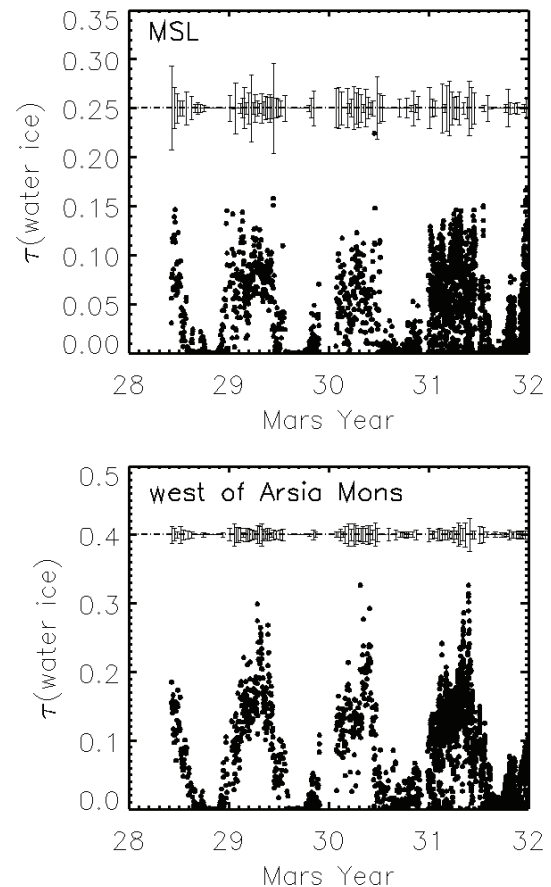


Figure 7. A time-series of MARCI water ice retrievals for: (top) 2×2 degree box centered on the MSL landing site; and (bottom) 2×2 degree box offset 1 degree west of the center of Arsia Mons. The “error bars” estimate the systematic retrieval error associated with the individual points (circles). The point-to-point scatter above this level represents the actual sol-to-sol variations in the water ice cloud column.

References: [1] Curran et al., 1973, *Journal of Geophysical Research*, 78, 4267; [2] Malin et al., 1992, *Journal of Geophysical Research*, 97, 7699; [3] Malin et al., 2008, *Icarus*, 194, 501. [4] Bell et al. 2009, *Journal of Geophysical Research (Planets)*, 114, E08S92; [5] Wolff et al. 2010, *Icarus*, 208, 143; [6] Wolff et al. 2011, *The Fourth International Workshop on the Mars Atmosphere*, 213-216; [7] Murchie et al., *Journal of Geophysical Research (Planets)*, 112, E05S03M; [8] Wolff et al., 2009, *Journal of Geophysical Research (Planets)*, 114, E00D04; [9] Smith, 2008, *Annual Review of Earth and Planetary Sciences*, 36, 191; [10] Thomas, et al., 1986, *Icarus*, 66, 39.